

RUGGED FLOW MORPHOLOGY OF LUNAR DOMES REVEALED BY EARTH-BASED RADAR. B. A. Campbell¹, B. R. Hawke², and D. B. Campbell³, ¹Center for Earth and Planetary Studies, Smithsonian Institution, Washington, DC 20560, campbellb@si.edu; ²HIGP, University of Hawaii, Honolulu, HI, 96822, hawke@higp.hawaii.edu; ³Cornell University, Ithaca, NY 14853, campbell@astro.cornell.edu.

Domes in the Marius Hills are spectroscopically similar to mare basalts, but new radar data show that these domes have backscatter strength comparable to near-rim ejecta from young craters, and circular polarization ratio values similar to blocky terrestrial volcanic deposits like SP flow in Arizona.

Introduction: Lunar basalt flow complexes, or maria, were initially smooth at the meter and larger scale. Evidence for eruptions of magma more viscous than the mare-forming flows, due either to slower eruption rates and associated cooling, increased initial silica content, or other mechanisms, is limited to a few clusters of flat-topped and sometimes steep-sided domes. The largest collection of such domes occurs in the Marius Hills region of Oceanus Procellarum. These volcanic constructs occupy a few-hundred meter high mare plateau, and appear to have formed in alternating episodes with the smoother surrounding flows [1]. Spectroscopic analysis suggests that the surfaces of the Marius domes are of similar composition to the mare units, while nearby cones and some smooth areas have signatures consistent with glass-rich materials that suggest a pyroclastic origin [1, 2]. The large-scale morphology of the domes is consistent with emplacement by more viscous lava. Most workers suggest, based on studies of lunar crustal melt evolution, that such increased viscosity arises due to eruptions of cooler, more crystalline basalt rather than more silica-rich magma [3].

Radar backscatter measurements can provide new information on the surface and near-surface physical properties of the Marius domes. Terrestrial basalt flows exhibit a range of surface morphology with either greater viscosity or local flow rate, from gently rolling pahoehoe structure to rugged, platy a'ā texture. In contrast, more silicic deposits, such as the basaltic-andesite SP flow in Arizona, can form blocky deposits made up of decimeter to meter-scale smooth-sided boulders. Radar measurements provide a means to indirectly measure the roughness of lava flow surfaces via the backscatter coefficient and ratios between echoes in different polarization states. Studies of terrestrial deposits show that blocky flows can have higher backscatter than a'ā flows [4, 5], properties used to infer that some lava flows on Mars have very rugged surfaces [6]. We present here new 12.6-cm and 70-cm wavelength Earth-based radar images and polarimetry data for the Marius Hills.

Radar Data: We transmit a left-circular-polarized signal from the Arecibo Observatory and receive both senses of the reflected echo from the Moon at the

Green Bank Telescope. The 70-cm data use a 3- μ s pulsed signal and 17-minute integration period to yield a spatial resolution of about 500 m per pixel. The 12.6-cm observations use a coded signal with a time resolution of 0.1 μ s and a 50-minute integration time to obtain a spatial resolution of about 25 m per pixel [7].

The observations capture the dynamic range of the lunar echoes and the receiver thermal noise. This allows for accurate calibration of the circular polarization ratio (μ_c or CPR), which is the ratio between the echo power in the same circular polarization sense (SC) as that transmitted to the echo power in the opposite circular sense (OC), $\mu_c = \sigma_{SC}^0 / \sigma_{OC}^0$. CPR values are used to measure the degree of single-bounce diffuse scattering from rough surfaces or multiple-bounce echoes from rugged but locally facet-like terrain. The dimensionless backscatter coefficient, σ^0 , is estimated via a number of steps, with a final uncertainty of ± 3 dB [7]. Across any single imaged area, however, the relative values of the backscatter strength are well calibrated. Comparisons to terrestrial features are enabled by data from the NASA/JPL AIRSAR, which collected multi-polarization measurements for many volcanic surfaces at 5.7-cm, 24-cm, and 68-cm wavelengths.

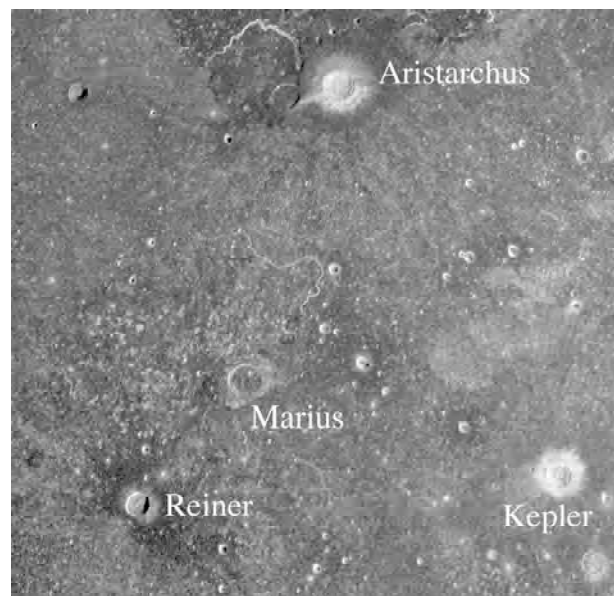


Fig. 1. SC polarization, 70-cm radar image. The Marius Hills form a pattern of high-backscatter patches N of Reiner and W and NW of Marius.

Radar Scattering Properties of the Marius Hills: The 12.6-cm radar data offer a high-resolution view of the scattering properties of the Marius domes. Except

for the bright radar reflections from the rims and walls of small pits and craters, there is little difference in SC backscatter at this wavelength between the maria and the domes. There is considerably more contrast in the circular polarization ratio, which is much higher on the domes than in the maria. The μ_c values for the domes are comparable to those observed around small impact craters in the maria, where the near-rim ejecta is rough at the 2-cm and larger scale that produces diffuse scattering at this wavelength. The 12.6-cm signals penetrate only about a meter, so the high CPR suggests that much more of the backscatter from the domes, relative to the maria, arises from diffuse or multiple scattering by surface or near-surface rocks.

Radar signals at 70-cm wavelength penetrate up to ~ 7 m in basaltic regolith, and backscatter from rocks of diameter ~ 10 cm and larger. The SC backscatter image shows that the Marius domes have greater contrast with the maria than observed at 12.6-cm wavelength (Fig. 1). Average values of the backscatter coefficient for sample regions within a single Arecibo illumination pattern show that σ^0 values for the Marius domes lie close to those for rough, near-rim ejecta deposits of Aristarchus and Cavalerius craters, and are a factor of ~ 10 higher than echoes from nearby mare flows.

The CPR enhancement from the domes is also more pronounced at 70-cm than at 12.6-cm wavelength, and we can compare these well-calibrated values among other imaged areas and with the AIRSAR data. SP flow has an average value of ~ 0.7 with little angular variation out to about 50° . Mare deposits have an average μ_c value of ~ 0.3 . Near-rim ejecta deposits of large impact craters have average CPR values that range from 0.5 for Cavalerius to 1.4 for Tycho. These differences are likely controlled by crater age more than by incidence angle, with younger craters having more 10-cm and larger blocks on and near the surface. The μ_c value presented for Tycho is an average over a 100-km^2 area, so local values can be even higher; a broad spread in local values is also noted for SP flow [4]. The Marius domes have average 70-cm CPR values from about 0.5 to 1.

Discussion and Interpretation: The Marius domes exhibit 70-cm radar scattering properties consistent with near-rim young crater ejecta, while at 12.6-cm the CPR remains high but the backscatter contrast with the maria is much smaller. The 70-cm CPR values of the Marius domes fall between those of terrestrial a'a flows and blocky deposits like SP flow, but do not reach the extreme values found for the Tycho crater near-rim ejecta blanket.

Circular polarization ratio values that approach or exceed unity can arise from coherent radar backscattering in thick deposits of water ice with internal cracks or voids [8]. Recent lunar observations, and earlier analyses of blocky terrestrial flows, show that high μ_c values are also possible in geologic settings where smooth-sided rocks are closely spaced at the

surface or comprise a dense population suspended within the probing range of the radar signal. The difference in CPR between such populations and (for example) an a'a flow may be due to small-scale roughness. Smooth-sided rocks act as facets that permit efficient double-bounce scattering, either between rocks or between the rocks and the surface. In contrast, an a'a flow offers no such locally smooth regions due to its jagged cm-scale structure. Each reflection reverses the sense of circular polarization, so a double-bounce event has a strong SC signature that may be further enhanced by the same coherent mechanism cited for internal scattering by ice.

The 70-cm scattering behavior of the Marius domes is consistent with a dense population of rocks, 10 cm and larger in diameter, either on the surface or within the probing depth of the radar (up to ~ 7 m). The lack of a major echo contrast between the domes and the nearby maria at 12.6-cm, however, suggests that most rocks are buried by some thickness of rock-poor material that more strongly attenuates the shorter-wavelength signal. The mare regolith is produced by impact fragmentation of an originally competent basalt layer to produce a mixture of rocks of varying diameter in a fine-grained matrix. Younger maria have thinner, more rocky regolith, and thus a higher σ_{sc}^0 and CPR for any given microwave loss characteristics [7]. Based on our survey of radar-bright and radar-dark maria, this process yields maximum 70-cm μ_c values of ~ 0.4 , below the range observed for the Marius domes. It thus appears unlikely that the radar scattering properties of the domes could arise by impact reworking of a smooth lava flow surface.

We conclude that the dome-forming flows had an initial morphology distinct from mare-forming units, and most likely similar to blocky terrestrial deposits like SP. The domes are not similar to the steep-sided "pancake" domes on Venus, which have relatively smooth upper surfaces and are inferred to form by slow extrusion of basalt [9]. If magma compositions with enhanced silica content are not plausible based on the lunar sample collection, then the blocky structure of the dome-forming lava must arise from some combination of compositional change, effusion rate, and/or cooling effects not typically observed in basaltic landforms on Earth.

References: [1] Heather D. J., et al., JGR., 108, 5017, doi:10.1029/2002JE001938, 2003. [2] Weitz, C. M., and J. W. Head, JGR, 104, 18,933-18,956, 1999 [3] Rutherford, M.J., et al., Proc. LPSC 5, 569-583, 1974. [4] Campbell, B.A. et al., JGR, 98, 17099-17114, 1993. [5] Plaut, J.J., et al., JGR, 109, doi:10.1029/2002JE002017, 2004. [6] Harmon, J.K., et al., JGR, 104, 14,065-14,090, 1999. [7] Campbell, B.A., et al., IEEE TGRS, 45, p.4032, 2007. [8] G. J. Black, et al., Icarus, vol. 151, pp. 167-180, 2001. [9] Stofan, E. R., et al., JGR., 105(E11), 26757-26772, 10.1029/1999JE001206, 2000.